J Chem Technol Biotechnol 80:68–75 (2005)
DOI: 10.1002/jctb.1159

Ozonation of CI Reactive Black 5 using rotating packed bed and stirred tank reactor

Yi-Hung Chen,[1] Ching-Yuan Chang,[1]* Wei-Ling Su,[1] Chun-Yu Chiu,[2] Yue-Hwa Yu,[1] Pen-Chi Chiang,[1] Chiung-Fen Chang,[1] Je-Lueng Shie,[1] Chyow-San Chiou[1] and Sally IM Chiang[3]

[1]*Graduate Institute of Environmental Engineering, National Taiwan University, Taipei 106, Taiwan*
[2]*Department of Environmental Engineering, Lan-Yang Institute of Technology, I-Lan 261, Taiwan*
[3]*Tairex Environmental Technology Co, Ltd, Taichung 420, Taiwan*

Abstract: This study investigates the ozonation of CI Reactive Black 5 (RB5) by using the rotating packed bed (RPB) and completely stirred tank reactor (CSTR) as ozone contactors. The RPB, which provides high gravitational force by adjusting the rotational speed, was employed as a novel ozone contactor. The same ozone dosage was separately introduced into either the RPB or the CSTR for the investigation, while the experimental solution was continuously circulated within the apparatus consisting of the RPB and CSTR. The decolorization and mineralization efficiencies of RB5 in the course of ozonation are compared for these two methods. Moreover, the dissolved and off-gas ozone concentrations were simultaneously monitored for the further analysis. As a result, the ozone mass transfer rate per unit volume of the RPB was significantly higher because of its higher mass transfer coefficient and gas–liquid concentration driving force. Furthermore, ozonation kinetics was found to be independent of the gravitational magnitude of an ozone gas–liquid contactor. Therefore, the results suggest employing RPBs as ozone-contacting devices with the advantage of volume reduction. The experimental results, which can be used for further modeling of the ozonation process in the RPB, also show the requirement of correct design for the RPB. Consequently, the present study is useful for the understanding of practical application of RPBs.

Keywords: rotating packed bed; ozonation; gas–liquid mass transfer; CI Reactive Black 5; high gravity; stirred tank reactor

NOTATION

a	Specific area of gas–liquid interface per unit volume of contactor ($m^2\ m^{-3}$)
a_p	Specific area of packing per unit volume of packed bed ($m^2\ m^{-3}$)
$Abs_{597.6}$	Absorbance at wavelength of 597.6 nm
ADMI	American Dye Manufacturer's Institute
C_{AGe}	Gas concentration of ozone of off-gas ($mg\ dm^{-3}$ or M)
C_{AGi}	Gas concentration of ozone of holdup gas ($mg\ dm^{-3}$ or M)
C_{AGi0}	Gas concentration of ozone of inlet gas ($mg\ dm^{-3}$ or M)
C_{ALb}	Dissolved ozone concentration in bulk liquid ($mg\ dm^{-3}$ or M)
C_{ALi}	Dissolved ozone concentration at gas-liquid interface ($mg\ dm^{-3}$ or M)
C_{B0}	Initial concentration of RB5 ($mg\ dm^{-3}$ or M)
C_i	Concentration of compound i in solution (M)
C_{TOC}	TOC concentration ($mg\ dm^{-3}$)
C_{TOC0}	Initial TOC concentration ($mg\ dm^{-3}$)
CSTR	Completely stirred tank reactor
CI	Colour Index
COD	Chemical oxygen demand ($mg\ dm^{-3}$)
d_p	Diameter of wire (m)
D_A	Liquid diffusion coefficient of ozone ($m^2\ s^{-1}$)
E_{rA}	Enhancement factor of ozone mass transfer
Ha	Hatta number, $(D_A \Sigma k_i C_i)^{0.5}/k^0_{LA}$
H_A	Henry's law constants of ozone, C_{AGi}/C_{ALi} ($M\ M^{-1}$)
k_d	Reaction rate constant of ozone self-decomposition (s^{-1})
k_i	Reaction rate coefficient for the ozonation of compound i ($M^{-1}s^{-1}$)
k^0_{LA}	Physical liquid-phase mass transfer coefficients of ozone ($m\ s^{-1}$)
m_{O_3A}	Applied ozone dosage defined by eqn (1) (mole)
m_{O_3R}	Amount of ozone consumption defined by eqn (3) (mole)
m_{O_3T}	Amount of ozone transferred by gas–liquid mass transfer defined by eqn (4) (mole)

* Correspondence to: Ching-Yuan Chang, Graduate Institute of Environmental Engineering, National Taiwan University, Taipei 106, Taiwan
E-mail: cychang3@ntu.edu.tw
(*Received 15 January 2004; revised version received 17 May 2004; accepted 12 August 2004*)
Published online 12 October 2004

Q_G	Gas flow rate ($dm^3\ s^{-1}$)
Q_L	Liquid flow rate ($dm^3\ min^{-1}$)
r	Radial position of packed bed (m)
r_1	Inner radius of packed bed (m)
r_2	Outer radius of packed bed (m)
r^2	Regression coefficient
RB5	Reactive Black 5
RPB	Rotating packed bed
t	Time (s)
TOC	Total organic carbon
V_H	Volume of gas holdup (dm^3)
V_L	Volume of liquid (dm^3)
V_R	Gas–liquid contacting volume (dm^3)
W_p	Weight of packing in packed bed (kg)
Z_B	Axial height of packed bed (m)
η_{TOC}	TOC removal efficiency defined by eqn (2) (%)
ρ_p	Density of wire ($kg\ m^{-3}$)

1 INTRODUCTION

Ozone is widely used as an oxidant in water and wastewater treatments. The ozone-containing gas generated from the ozone generator is transferred to water by introducing it through the gas–liquid contactor. The common advantages of ozonation are to increase the decolorization, mineralization and biodegradability of the solution.[1,2] Furthermore, the rate-limiting step in many ozonation processes is attributed to the gas–liquid mass transfer rate.[3–5] It indicates that the ozonation performance can be enhanced by increasing the gas–liquid mass transfer rate of ozone. Consequently, the innovation of an ozone-contacting device with better mass transfer efficiency is desirable.

Rotating packed beds (RPBs) have been used as gas–liquid contactors for the applications of adsorption, distillation and stripping, etc.[6–8] RPBs are designed to generate high acceleration of liquid owing to the centrifugal force. The target solution contacted with gas flows through the packed material in the environment of high gravity. This novel technology is also named 'Higee'. According to previous studies,[6–12] RPBs have high gas–liquid mass transfer coefficients, which are important for increasing the gas–liquid mass transfer rate. Recently, RPBs have been introduced as ozonation contactors by Lin and Liu[13] and Chen *et al*.[14] Their studies investigated the effects of operating variables on the ozonation in RPBs. It is still essential, however, to compare the ozonation process using the RPB with that using the convectional contactors such as the completely stirred tank reactor (CSTR). The comparison would clarify the advantages of mass transfer properties and the possible difference of ozonation dynamics for ozone gas–liquid mass transfer combined with reactions of pollutants in an RPB.

This study employs the RPB and CSTR separately as the ozonation contactor to treat the reactive dyes of the textile. The reactive dyes, which are predominant in the application of dyes, have significant impacts upon the conventional methods of wastewater treatments due to their poor biodegradability, especially those containing azo-groups.[15,16] The CI Reactive Black 5 (RB5) is one of the common reactive dyes and was chosen as a target pollutant. The experimental solution of 5.5 dm^3 was continuously circulated within the apparatus consisting of the RPB and CSTR, while the same ozone dosage was separately introduced into either the RPB or the CSTR for comparison. The removal of the absorbance, ADMI value and total organic carbon (TOC) concentration are measured in the course of RB5 ozonation. Moreover, the dissolved and off-gas ozone concentrations are simultaneously monitored for further analysis.

As a result, the ozone mass transfer rate per unit volume of the RPB was found to be remarkably higher than that of the CSTR. This can be attributed to the higher mass transfer coefficient and gas–liquid concentration driving force in the RPB. Furthermore, the ozonation kinetics of RB5 was examined and compared with the uses of these two types of ozone gas contactors. The ozonation of RB5, however, seems to be better when in ozone is introduced into the CSTR due to its significantly larger volume than the RPB in this study. Consequently, the use of an RPB was considered advantageous to reduce the volume of an ozone contactor. This study provides useful information about the application of an RPB in ozonation processes.

2 EXPERIMENTAL

2.1 Materials

The RB5, chemical formula $C_{25}H_{26}N_5O_{19}S_6{\cdot}4Na$, was purchased from Aldrich Chemical Company (Amherst, NY, USA); it was of 55% purity, and had a molecular weight of 991.8. The characteristic wavelength of absorbance of RB5 is 597.6 nm, which is responsible for the dark blue color arising from aromatic rings connected by azo groups. The prescription of RB5 concentration (C_{B0}) as the sole organic target was 100 $mg\ dm^{-3}$ with the initial TOC concentration (C_{TOC0}) of about 24.6 $mg\ dm^{-3}$. The initial pH value of the solution was 8.3. All experimental solutions were prepared with deionized water. No other chemical, as scavenger or promoter, was added to the solution.

2.2 Ozone gas–liquid contactors

Figure 1 shows a simple description of an RPB, which consists of a rotator and a stationary case. The 304 stainless steel wire wrapped in the shape of annular rings is stacked in the packed bed. The density (ρ_p) and diameter (d_p) of the wire are 8478 $kg\ m^{-3}$ and 2.2×10^{-4} m, respectively. The rotator is connected to a rotor shaft on two bearings, which are in turn mounted on a steel structure. The shaft is connected to a motor, which is controlled by a speed regulator. The rotational speed is controlled at 1500 rpm, which provides gravitational force of 103 g based on

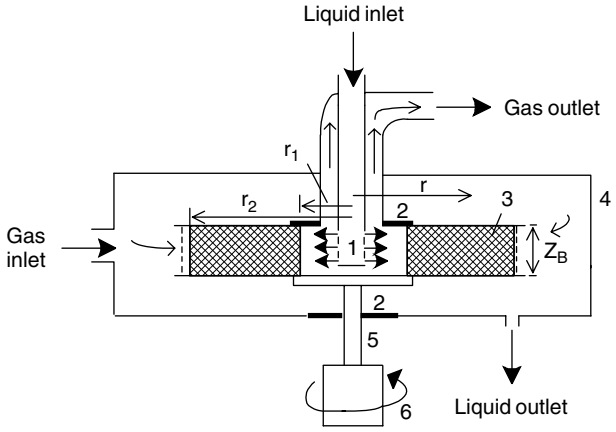

Figure 1. Schematic diagram of RPB contactor. Components: 1, stationary liquid distributor; 2, seal; 3, packed bed rotator; 4, housing case; 5, rotor shaft; 6, motor.

Table 1. Specification of RPB contactor used in this study

Item	Unit	Value
Inner radius of packed bed, r_1	m	0.023
Outer radius of packed bed, r_2	m	0.059
Axial height of packed bed, Z_B	m	0.02
Weight of packing in packed bed, W_p	kg	0.0686
Volume of gas-liquid contacting, V_R	dm^3	0.185
Volume of housing case	dm^3	1.04
Specific area of packing per unit volume of packed bed, a_p	$m^2\,m^{-3}$	793
Total packing area, $a_p \times V_R$	m^2	0.147
Voidage of packed bed	$m^3\,m^{-3}$	0.956

the arithmetic mean radius of the RPB. Liquid enters the RPB through six holes in the liquid distributor. These six holes are arranged in two vertical groups of three per group with groups spaced 180° apart. The liquid is sprayed on the inside edge of the RPB and thrown outwards by the centrifugal force. The gas is introduced from the outside and flows counter-currently with respect to the liquid in the RPB. The specification of the RPB contactor is given in Table 1.

The CSTR of 17.2 cm inside diameter, volume 5.5 dm^3, is made of Pyrex glass and equipped with a water jacket to maintain a constant solution temperature of 25 °C in all experiments. The design of the CSTR is based on the criteria of the shape factors of a standard six-blade turbine.[17] The stirring speed is as high as 800 rpm to ensure complete mixing, based on the results of previous tests.[18,19] The gas diffuser, of cylindrical shape with the pore size of 10 μm, is located at the bottom of the CSTR. Note that the gas–liquid contacting volume (V_R) in the CSTR (5.5 dm^3) is about 30 times that in the RPB (0.185 dm^3) due to the small dimensions of the RPB. In addition, the V_R, specific area of packing (a_p) and voidage of packed bed are determined as $\pi Z_B(r_2{}^2 - r_1{}^2)$, $4W_p/(d_p V_R \rho_p)$ and $1 - W_p/(V_R \rho_p)$, respectively.

2.3 Analytical

The color of the RB5 solution is measured by both the absorbance of characteristic wavelength ($Abs_{597.6}$) and an ADMI method. The optical spectra (200–900 nm) in UV-visible absorption are scanned by the UV-visible spectrometer (model Cintra 20, GBC, Dandenong, VIC, Australia). The pH value is continuously monitored by the pH meter (model 300T, Suntex, Taipei, Taiwan) with a glass probe sensor. The TOC concentration (C_{TOC}) of the sample is analyzed by a TOC analyzer (model 700, OI Corporation, Texas, USA). The instrument utilizes the UV-persulfate technique to convert the organic carbon for the subsequent analysis by an infrared carbon dioxide analyzer calibrated with the potassium hydrogen phthalate standard. Moreover, the dissolved ozone concentration (C_{ALb}) is measured instantly by the liquid ozone monitor (model 3600, Orbisphere Lab, Neuchâtel, Switzerland) with a sensor of membrane-containing cathode.

2.4 Experimental procedures

Ozone-containing gas generated from pure oxygen by the ozone generator (Tairex Environmental Technology, Taiwan) is introduced into RPB and CSTR separately with the gas flow rate (Q_G) of 0.0323 $dm^3\,s^{-1}$. Before starting the ozonation experiments, the ozone gas is bypassed to the photometric analyzer (model SOZ-6004, Seki, Tokyo, Japan) to assure the stability of the fed ozone concentration (C_{AGi0}) as 30 mg dm^{-3}. Then, the gas stream at the preset flow rate is directed into the contactor when reaching the set conditions. The total experimental solution of 5.5 dm^3 (V_L) is circulated between the CSTR and RPB continuously with the flow rate (Q_L) of 0.6 $dm^3\,min^{-1}$. The same applied ozone dosage (m_{O_3A}) for the RPB or CSTR is defined in eqn (1).

$$m_{O_3A} = Q_G \times C_{AGi0} \times t \tag{1}$$

Liquid samples are drawn out from the CSTR at desired time intervals in the course of experiments to analyze their properties. The residual dissolved ozone in the samples is removed by stripping with nitrogen. According to the test results, the residual dissolved ozone with the initial value of 5 mg dm^{-3} can be stripped by nitrogen with more than 98% removed (below 0.1 mg dm^{-3}) within 30 s and complete removal within 60 s from the solution, which is determined by the indigo method with the detection limit of 0.01 mg dm^{-3}. The sample volume and nitrogen flow rate are 20 cm^3 and 0.0167 $dm^3\,s^{-1}$, respectively. For the ozonation regime with negligible residual dissolved ozone, the sampling time interval does not affect the measurements of absorbance and TOC of solution. In the ozonation regime with significant residual dissolved ozone, the sampling time interval should be longer, say 10 min, in order to reduce the lag effect of nitrogen stripping. For the sampling time interval of 10 min, the lag effect of quenching the ozonation reaction on the experimental results is less than 5% (estimated by noting that

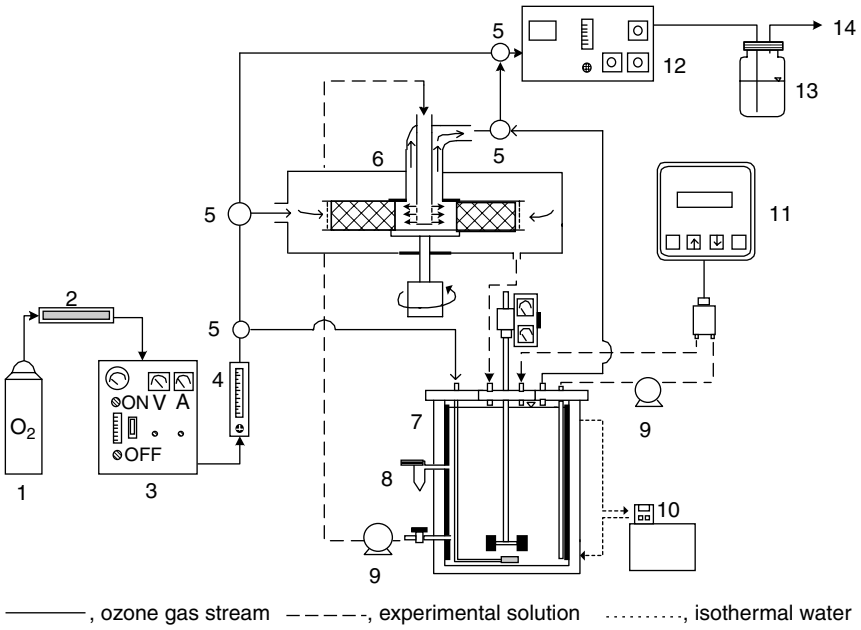

Figure 2. Experimental apparatus sketch. Components: 1, oxygen cylinder; 2, drying tube; 3, ozone generator; 4, flow meter; 5, three-way valves; 6, rotating packed bed gas–liquid contactor; 7, stirred reactor; 8, sample port; 9, pumps; 10, thermostat; 11, liquid ozone monitor; 12, gaseous ozone detector; 13, KI solution; 14, vent to hood.

30 s/10 min is about 5%) and may be tolerable. Thus, the results are presented with the ozonation time intervals as noted above. In addition, a circulation pump is used to transport the liquid from the CSTR to the sensor of dissolved ozone monitor with a flow rate of 0.18 dm^3 min^{-1}, and to reflow it back during the ozonation. All the experiments are carried out repeatedly to guarantee the accuracy of the obtained data. From the study of Chen *et al*,[14] the Henry's constant (H_A) and volumetric mass transfer coefficient of ozone (k^0_{LA} a) in the RPB are 4.18 and 0.0975 s^{-1}, respectively. The experimental apparatus employed in this work is illustrated in Fig 2.

3 RESULTS AND DISCUSSION

3.1 Decolorization and mineralization of RB5 by ozonation

The initial values of $Abs_{597.6}$ and ADMI for the RB5 solution were 2.69 and 1620 units, respectively. As shown in Fig 3, the reductions of $Abs_{597.6}$ and ADMI remarkably increase with ozonation time to reach 100%, because the first attack of ozone on RB5 is through the cleavage of dye chromophores, resulting in the reduction of absorbance in visible wavelengths, which are characterized by an N=N bond.[20] In addition, the variations of $Abs_{597.6}$ and ADMI (which is calculated from the absorbances at 438, 540 and 590 nm) show similar trends under the same condition of ozone introduction, which indicates the consistent reductions of absorbances in these characteristic wavelengths during the ozonation of RB5. Furthermore, the efficiency of decolorization is obviously greater with the introduction of ozone into the CSTR. The time required for 99% removal of color is about 10 and 30 min by introducing ozone into the CSTR and RPB, respectively.

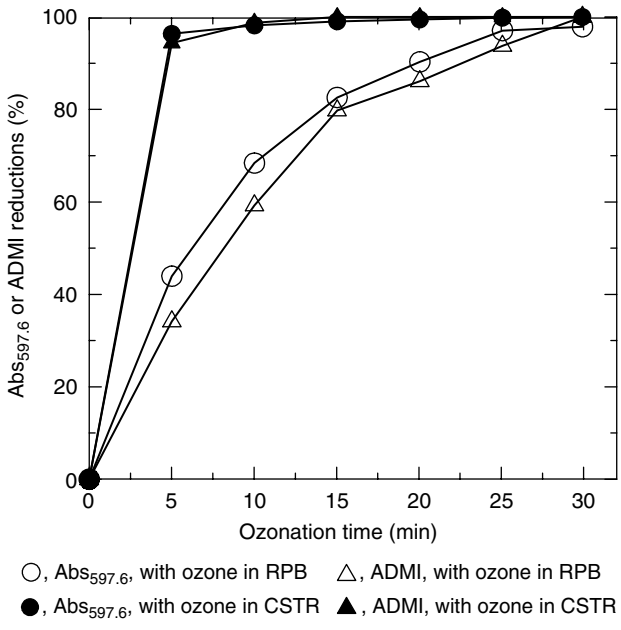

Figure 3. Variations of $Abs_{597.6}$ and ADMI reductions with time for the ozonation of RB5.

In terms of mineralization of the RB5 solution, the variations of the normalized TOC concentration (C_{TOC}/C_{TOC0}) are shown in Fig 4. The TOC of the solution is reduced by 41% (at 90 min) and 60% (at 100 min) by using the RPB and CSTR as the ozone contactors, respectively. Apparently, the mineralization rate is slower than the decolorization rate. This can be explained in terms of the degradation of the parent compound's aromatic rings which lags behind that of the chromophores. Another cause is

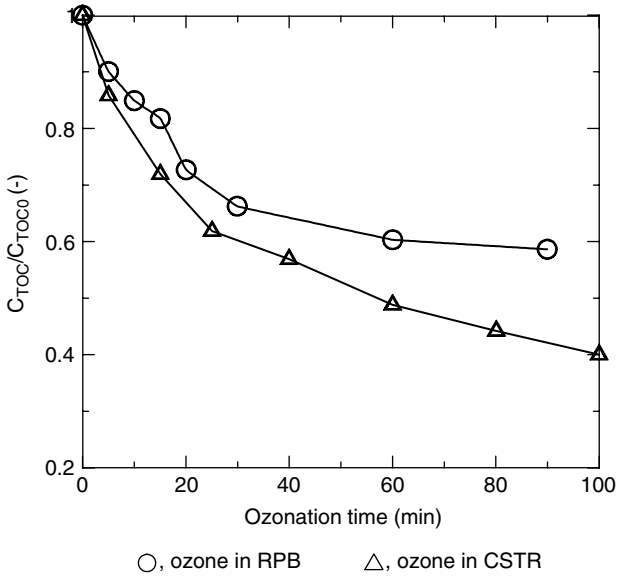

Figure 4. Variation of C_{TOC}/C_{TOC0} with time for the ozonation of RB5. $C_{TOC} = C_{TOC0}$ at $t = 0$.

that the intermediates containing organic carbons are resistant toward further oxidation. This explanation is consistent with the experimental results of other azo dyes reported by Alvares *et al*[20] who observed a lag of COD removal behind the decolorization. Additionally, the elimination rate of TOC, C_{TOC}, was also found to be faster when introducing ozone into the CSTR compared with introducing it into the RPB.

Moreover, the variations of dissolved (C_{ALb}) and off-gas (C_{AGe}) ozone concentrations were analyzed to examine the consumption of ozone, which is related to the solution reactivity in the course of ozonation of RB5 (Fig 5). The C_{ALb} remained almost undetectable in the early period of ozonation, while the C_{AGe} increased gradually with ozonation time. The higher C_{AGe} value of the RPB reveals its overall lower ozone utilization for ozonation times <27 min. In this early stage, the reactivity of the solution is high and the ozone transferred from the fed gas into solution (C_{ALb}) is consumed immediately. Afterwards the C_{ALb} value starts to increase in the liquid phase, indicating the lower reactivity of the solution in the later ozonation stage. Then both C_{AGe} and C_{ALb} approach to the steady values of about 27 and 5 mg dm^{-3}, respectively. It is observed that the increase in the C_{ALb} value started earlier and increased faster with the introduction of ozone into the CSTR compared with the RPB results. Hence, according to the results of decolorization, mineralization and ozone accumulation, the ozonation of RB5 progresses faster by employing the CSTR as the ozone contactor.

3.2 Comparison of ozonation processes with ozone gas introduced in the RPB and CSTR

The dissimilar ozonation performance may be caused by different ozone gas–liquid mass transfer rates. Therefore, further examination was made to distinguish the mass transfer characteristics of these

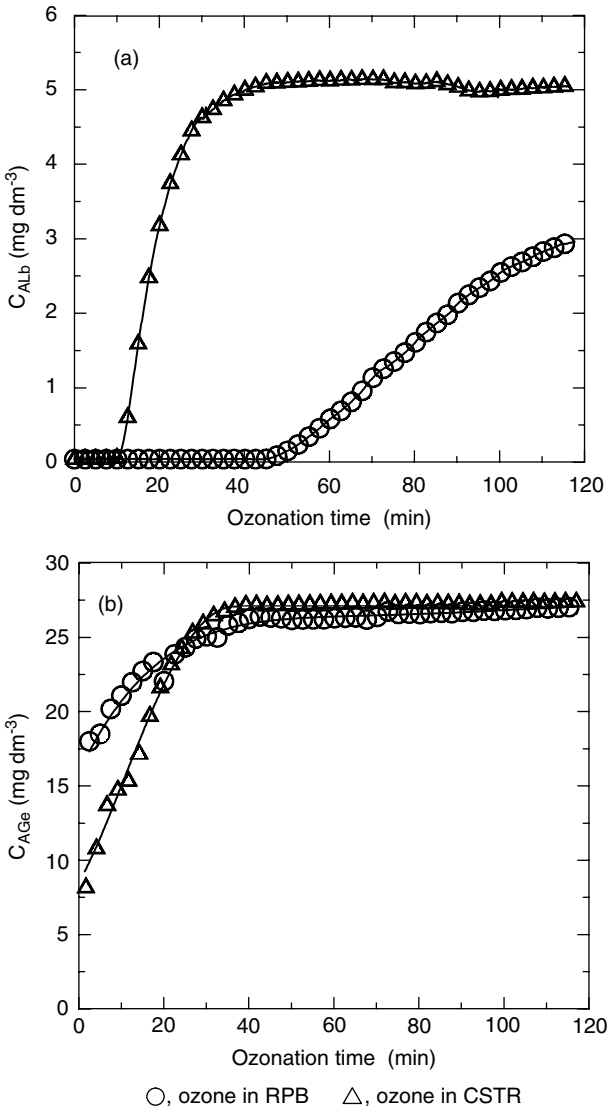

Figure 5. Variations of C_{ALb} (a) and C_{AGe} (b) with time for the ozonation of RB5.

two contactors. As for different ozonation kinetics and mechanisms, variation in mineralization efficiency could be observed with the same ozone consumption. Accordingly, the dependence of TOC removal efficiency (η_{TOC}) on the amount of ozone consumption (m_{O_3R}) was examined during the ozonation of RB5. The η_{TOC} and m_{O_3R} are defined by eqns (2) and (3), respectively.

$$\eta_{TOC} = (C_{TOC0} - C_{TOC})/C_{TOC0} \tag{2}$$

$$\begin{aligned} m_{O_3R} &= \text{ozone applied} - \text{ozone exited} - \text{ozone accumulated in holdup gas and liquid} \\ &= \int_0^t Q_G(C_{AGi0} - C_{AGe})dt - C_{AGi}V_H - C_{ALb}V_L \end{aligned} \tag{3}$$

In eqn (3), C_{AGi} is the ozone concentration in holdup gas of the contactor, and taken as C_{AGe} in the calculation for simplicity, and V_H is the volume of holdup gas in the contactor. As shown in Fig 6, the extent

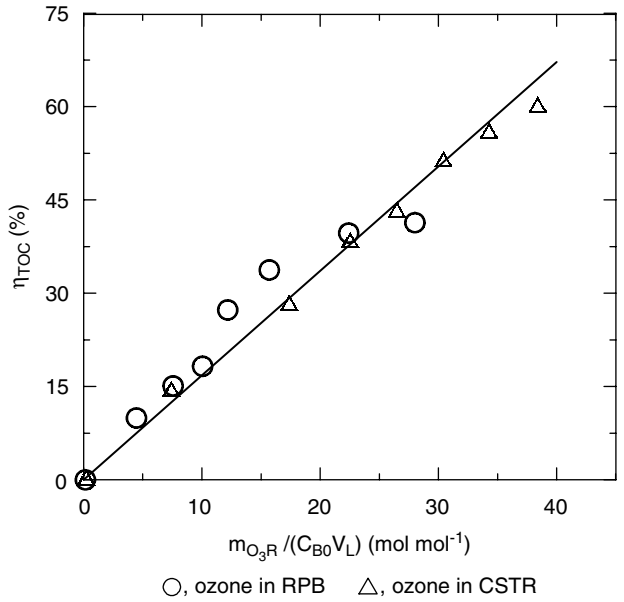

Figure 6. η_{TOC} vs $m_{O_3R}/(C_{B0}V_L)$ for the ozonation of RB5. Line: the plot of correlation equation of $\eta_{TOC}(\%) = 1.68\, m_{O_3R}/(C_{B0}V_L)$ (mol mol^{-1}) with $r^2 = 0.958$.

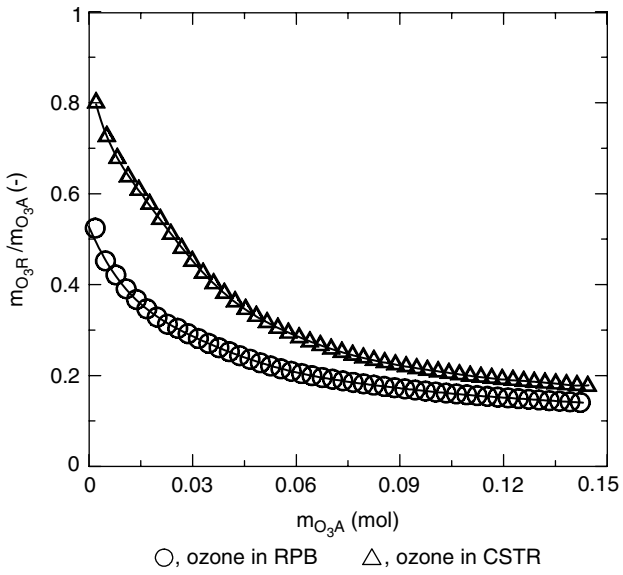

Figure 7. m_{O_3R}/m_{O_3A} vs m_{O_3A} for the ozonation of RB5.

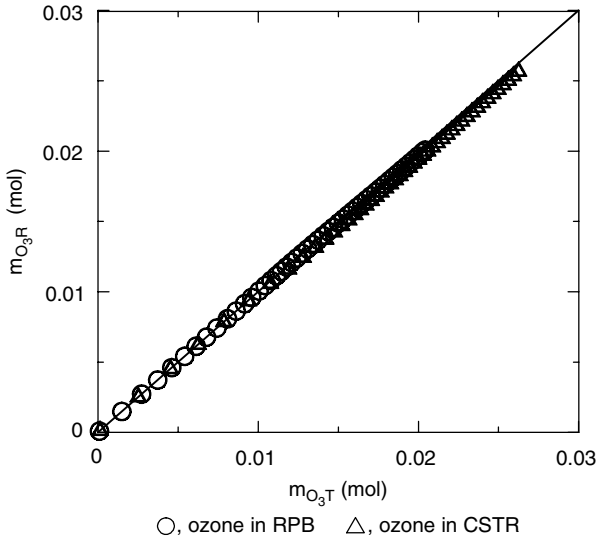

Figure 8. m_{O_3R} vs m_{O_3T} for the ozonation of RB5.

of mineralization of the solution apparently and consistently depends on the value of $m_{O_3R}/(C_{B0}V_L)$ for these two contactors. The equation of $\eta_{TOC}(\%) = 1.68\, m_{O_3R}/(C_{B0}V_L)$ (mol mol^{-1}) is presented, with $r^2 = 0.958$. The ozonation mechanism of the pollutant in the RPB is the same as that in the CSTR. Fig 6 shows that the ozonation kinetics is independent of the gravitational magnitude of ozone gas–liquid contactors. Accordingly, the ozonation kinetics obtained from other kinds of ozonation reactors can be directly applied for the RPB contactor.

The pH value of solution slightly increases from 8.3 to 8.7 during the ozonation. The radical ozonation, which is more non-selective toward the pollutant elimination, would be enhanced at higher pH values by the generation of hydroxyl radicals from ozone decomposition.[21] In Fig 5, the steady ozone concentrations in the later period reveal that the consumption of ozone in the experimental conditions of this study mainly resulted from the self-decomposition of ozone, while the TOC content of the solution was still noticeable and decreasing. The reaction rate constant of ozone self-decomposition (k_d) can be calculated as 0.00 332 s^{-1} by employing $k_d = Q_G(C_{AGi0} - C_{AGe})/(V_L C_{ALb})$ with the steady state values of C_{AGe}(27.2 mg dm^{-3}) and C_{ALb}(5.0 mg dm^{-3}). This k_d value in the basic condition at pH = 8.3–8.7 is evidently greater than that of 0.000 145 s^{-1} at pH = 5.25. Furthermore, the approximately linear relationship of η_{TOC} with $m_{O_3R}/(C_{B0}V_L)$ as shown in Fig 6 also supports that the contribution of the radical ozonation on the elimination of RB5 is significant.

In addition, the ratio of consumed to applied ozone (m_{O_3R}/m_{O_3A}) is used as a quantitative indicator to represent the ozone utilization, as depicted in Fig 7. The m_{O_3R}/m_{O_3A} value decreases with m_{O_3A} from 0.52 to 0.14 and 0.80 to 0.18 for the cases with RPB and CSTR as ozone contactors, respectively. The decreasing m_{O_3R}/m_{O_3A} value may be caused by the lower reactivity of the reacted solution and the accumulation of dissolved ozone. Evidently, the m_{O_3R}/m_{O_3A} value was apparently lower at the same m_{O_3A} when using the RPB as the ozone contactor. The ozone utilization increased 24–67% as ozone was introduced into the CSTR. This phenomenon caused the difference of overall ozonation performance between the two cases.

Figure 8 shows that the m_{O_3R} value was slightly lower than the amount of ozone transferred (m_{O_3T}) by the gas–liquid mass transfer. The m_{O_3T} is defined by the double integration of the specific gas–liquid mass transfer rate, $E_{rA}k^0_{LA}a\,(C_{AGi}/H_A - C_{ALb})$, with respect to the volume of gas–liquid contactor and time, as

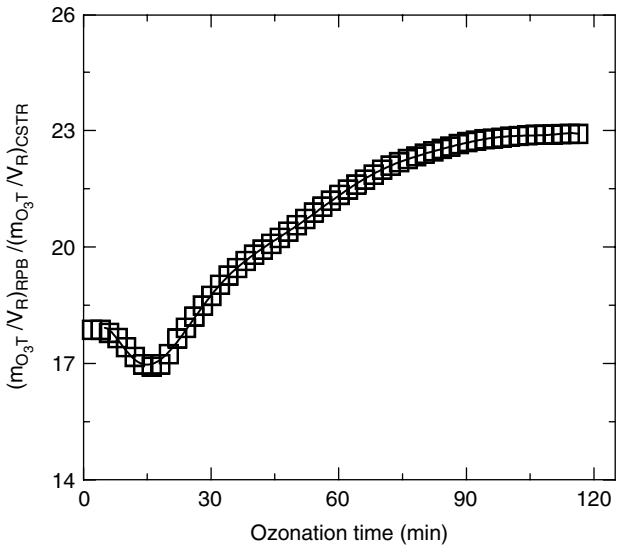

Figure 9. Variation of $(m_{O_3T}/V_R)_{RPB}/(m_{O_3T}/V_R)_{CSTR}$ with time for the ozonation of RB5.

shown in eqn (4).

$$\begin{aligned} m_{O_3T} &= \int_0^t \int_0^{V_R} E_{rA} k_{LA}^0 a (C_{AGi}/H_A - C_{ALb}) \mathrm{d}V \mathrm{d}t \\ &= \text{ozone applied} - \text{ozone exited} - \text{ozone} \\ &\quad \text{accumulated in holdup gas} \\ &= \int_0^t Q_G (C_{AGi0} - C_{AGe}) \mathrm{d}t - C_{AGi} V_H \end{aligned} \tag{4}$$

In eqn (4), E_{rA} is the enhancement factor of ozone gas–liquid mass transfer. As a result, the better ozonation performance of the CSTR is due to its higher m_{O_3T} value.

Further, the average amount of ozone transferred by gas–liquid mass transfer per unit gas–liquid contacting volume, m_{O_3T}/V_R, for these two contactors were calculated respectively for the comparison. As shown in Fig 9, the variation of the ratio of the values of m_{O_3T}/V_R of RPB to CSTR with ozonation time ranged between 17 and 23. Based on eqn (4), the m_{O_3T}/V_R depends on the E_{rA}, $k_{LA}^0 a$, gas–liquid concentration driving force $(C_{AGi}/H_A - C_{ALb})$ and t; the E_{rA} depends on the value of the Hatta number $(Ha = \sqrt{D_A \Sigma k_i C_i}/k_{LA}^0)$,[3,4] which is inversely proportional to the k_{LA}^0. Referring to previous studies, the k_{LA}^0 values of the RPB $(2.97 \times 10^{-5}–1.32 \times 10^{-4}\,\mathrm{m\,s^{-1}})$[14] and CSTRs $(4.75 \times 10^{-5}–2.32 \times 10^{-4}\,\mathrm{m\,s^{-1}})$[3,4,22] were found to be in the same order of magnitude. Accordingly, the E_{rA} value may not be significantly different for these two contactors. Therefore, the larger value of ratio of $(m_{O_3T}/V_R)_{RPB}/(m_{O_3T}/V_R)_{CSTR}$ is mainly attributed to the difference of $k_{LA}^0 a$ and $C_{AGi}/H_A - C_{ALb}$. The $k_{LA}^0 a$ value in the RPB $(0.0975\,\mathrm{s^{-1}})$ is apparently higher than that in the CSTR $(0.02–0.04\,\mathrm{s^{-1}})$ reported by Zaror.[23] In this study, the $k_{LA}^0 a$ value in the CSTR was $0.0248\,\mathrm{s^{-1}}$. Moreover, the ratio of the values of $C_{AGi}/H_A - C_{ALb}$ in the RPB to the CSTR was approximately estimated to be about 3.1 computed from the average values of $C_{AGe}/H_A - C_{ALb}$ in Fig 5. Additionally, the hydrodynamics of the RPB is close to plug flow, which is more beneficial for a higher gas–liquid concentration driving force because of the higher ozone concentration gradient profiles.[24] The better ozonation performance by using the CSTR in this study may be attributed to its larger volume. Certainly, the comparison of ozonation performance in a CSTR with that in a RPB of the same volume would be helpful to further support this point.

Consequently, it is feasible to reduce the volume of an ozone gas–liquid contactor by employing RPBs based on the above analysis. It is worthy of mention that the further modeling and pilot test are helpful in the correct design of the size and dimensions of the RPB. The experimental data obtained in this study can be used to establish the ozonation model for using a RPB gas–liquid contactor.

4 CONCLUSIONS

The rotating packed bed (RPB) and completely stirred tank reactor (CSTR) are compared as an ozone gas–liquid contactor to treat CI Reactive Black 5 (RB5). During the ozonation course of RB5, both the absorbance of characteristic wavelength and ADMI value decreased quickly and similarly to zero. The mineralization rate of RB5 was significantly slower than the decolorization rate because of the selective attack of ozone and low reactivity of intermediates. The removal efficiency of TOC (%) was proportional to the ratio $(\mathrm{mol\,mol^{-1}})$ of moles of consumed ozone to that of treated RB5 with the pre-multiplying coefficient of 1.68. Furthermore, the ozonation kinetics obtained elsewhere can be applied adequately for the RPB system. Note that the mass transfer rate of ozone per unit volume in the RPB gas–liquid contactor was significantly higher because of its higher volumetric mass transfer coefficient $(k_{LA}^0 a = 0.0975\,\mathrm{s^{-1}})$ and gas–liquid concentration driving force as compared with the CSTR gas–liquid contactor $(k_{LA}^0 a = 0.0248\,\mathrm{s^{-1}})$. The enhancement factor of ozone gas–liquid mass transfer may not have significant difference between the RPB and the CSTR. As a result, it is feasible to reduce the volume of an ozone gas–liquid contactor by using a RPB, while the correct design of the size and dimensions of the RPB is required.

REFERENCES

1 Hong PKA and Zeng Y, Degradation of pentachlorophenol by ozonation and biodegradability of intermediates. *Water Res* **36**:4243–4254 (2002).

2 Sevimli MF and Sarikaya HZ, Ozone treatment of textile effluents and dyes: effect of applied ozone dose, pH and dye concentration. *J Chem Technol Biotechnol* 77:842–850 (2002).

3 Beltrán FJ, Encinar JM and Garcia-Araya JF, Ozonation of *o*-cresol in aqueous solutions. *Water Res* **24**:1309–1316 (1990).

4 Beltran-Heredia J, Torregrosa J, Dominguez JR and Peres JA, Kinetics of the reaction between ozone and phenolic acids present in agro-industrial wastewaters. *Water Res* **35**:1077–1085 (2001).
5 Qiu YQ, Kuo CH and Zappi ME, Performance and simulation of ozone absorption and reactions in a stirred-tank reactor. *Environ Sci Technol* **35**:209–215 (2001).
6 Ramshaw C and Mallinson RH, Mass transfer process. US Patent 4 283 255 (1981).
7 Singh SP, Wilson JH, Counce RM, Villiers-Fisher JF, Jennings HL, Lucero AJ, Reed GD, Ashworth RA and Elliott MG, Removal of volatile organic compounds from groundwater using a rotary air stripper. *Ind Eng Chem Res* **31**:574–580 (1992).
8 Liu HS, Lin CC, Wu SC and Hsu HW, Characteristics of a rotating packed bed. *Ind Eng Chem Res* **35**:3590–3596 (1996).
9 Tung HH and Mah RSH, Modeling liquid mass transfer in higee separation process. *Chem Eng Commun* **39**:147–153 (1985).
10 Keyvani M and Gardner NC, Operating characteristics of rotating beds. *Chem Eng Prog* **85**:48–52 (1989).
11 Munjal S, Dudukovic MP and Ramachandran P, Mass-transfer in rotating packed beds—I. Development of gas–liquid and liquid–solid mass-transfer correlations. *Chem Eng Sci* **44**:2245–2255 (1989).
12 Kumar MP and Rao DP, Studies on a high-gravity gas–liquid contactor. *Ind Eng Chem Res* **29**:917–920 (1990).
13 Lin CC and Liu WT, Ozone oxidation in a rotating packed bed. *J Chem Technol Biotechnol* **78**:138–141 (2003).
14 Chen YH, Chang CY, Su WL, Chen CC, Chiu CY, Yu YH, Chiang PC and Chiang SIM, Modeling ozone contacting process in a rotating packed bed. *Ind Eng Chem Res* **43**:228–236 (2004).
15 Churchley JH, Ozone for dye waste color removal: four years operation at Leek STW. *Ozone Sci Eng* **20**:111–120 (1998).
16 Ince NH and Tezcanlí G, Reactive dyestuff degradation by combined sonolysis and ozonation. *Dyes and Pigments* **49**:145–153 (2001).
17 McCabe WL, Smith JC and Harriott P, *Unit Operations of Chemical Engineering*. McGraw-Hill, New York, NY, USA (1993).
18 Li H, Chang CY, Chiu CY, Yu YH, Chiang PC, Chen YH, Lee SJ, Ku Y and Chen JN, Kinetics of ozonation of polyethylene glycol in printed wiring board electroplating solution. *J Chinese Ints Environ Eng (Taiwan)* **10**:69–75 (2000).
19 Chang CY, Chen YH, Li H, Chiu CY, Yu YH, Chiang PC, Ku Y and Chen JN, Kinetics of decomposition of polyethylene glycol in electroplating solution by ozonation with UV radiation. *J Environ Eng-ASCE* **127**:908–915 (2001).
20 Alvares ABC, Diaper C and Parsons SA, Partial oxidation of hydrolysed and unhydrolysed textile azo dyes by ozone and the effect on biodegradability. *Trans IChemE* **79**:103–108 (2001).
21 Zeng Y, Hong PKA and Wavrek DA, Chemical–biological treatment of pyrene. *Water Res* **34**:1157–1172 (2000).
22 Chiu CY, Chang CY, Huang WH, Lee SJ, Yu YH, Liou HT, Ku Y and Chen JN, A refined model for ozone mass transfer in a semibatch stirred vessel. *Ozone Sci Eng* **19**:439–456 (1997).
23 Zaror CA, Enhanced oxidation of toxic effluents using simultaneous ozonation and activated carbon treatment. *J Chem Technol Biotechnol* **70**:21–28 (1997).
24 Chen YH, Chang CY, Chiu CY, Yu YH, Chiang PC, Ku Y and Chen JN, Dynamic behavior of ozonation with pollutant in a countercurrent bubble column with oxygen mass transfer. *Water Res* **37**:2583–2594 (2003).